MethodsX 8 (2021) 101247

Contents lists available at ScienceDirect

MethodsX

journal homepage: www.elsevier.com/locate/mex

Method Article

The method to quantify cell elasticity based on the precise measurement of pressure inducing cell deformation in microfluidic channels

Zhenlin Chen[a], Tsz Fung Yip[b,c], Yonggang Zhu[a], Joshua W.K. Ho[b,c,*], Huaying Chen[a,*]

[a] School of Mechanical Engineering and Automation, Harbin Institute of Technology, Shenzhen, Shenzhen 518055, China
[b] School of Biomedical Sciences, Li Ka Shing Faculty of Medicine, The University of Hong Kong, Pokfulam Hong Kong, China
[c] Laboratory of Data Discovery for Health Limited (D24H), Hong Kong Science Park, New Territory, Hong Kong, China

A B S T R A C T

The cell elasticity has attracted extensive research interests since it not only provides new insights into cell biology but also is an emerging mechanical marker for the diagnosis of some diseases. This paper reports the method for the precise measurement of mechanical properties of single cells deformed to a large extent using a novel microfluidic system integrated with a pressure feedback system and small particle separation unit. The particle separation system was employed to avoid the blockage of the cell deformation channel to enhance the measurement throughput. This system is of remarkable application potential in the precise evaluation of cell mechanical properties. In brief, this paper reports:

- The manufacturing of the chip using standard soft lithography;
- The methods to deform single cells in a microchannel and measure the relevant pressure drop using a pressure sensor connecting to the microfluidic chip;
- Calculation of the mechanical properties including stiffness and fluidity of each cell based on a power-law rheology model describing the viscoelastic behaviors of cells;
- Automatic and real-time measurement of the mechanical properties using video processing software.

A R T I C L E I N F O

Method name: The method to quantify cell elasticity based on the precise measurement of pressure inducing cell deformation in microfluidic channels
Keywords: Cell elasticity, Measurement, Microfluidic, Pressure drop, Cell deformation, Video processing
Article history: Available online 23 January 2021

* Corresponding authors.
E-mail addresses: jwkho@hku.hk (J.W.K. Ho), chenhuaying@hit.edu.cn (H. Chen).

https://doi.org/10.1016/j.mex.2021.101247

Specifications table

Subject Area:	Engineering
More specific subject area:	*Cell elasticity measurement*
Method name:	*The method to quantify cell elasticity based on the precise measurement of pressure inducing cell deformation in microfluidic channels*
Name and reference of original method:	*Z. Chen, Y. Zhu, D. Xu, M. M. Alam,* L. *Shui and H. Chen, Cell elasticity measurement using a microfluidic device with real-time pressure feedback. Lab on a Chip, 2020, 20, 2343–2353.*
Resource availability:	

Method details

Background

The mechanical properties of cells are closely related to not only their biological functions, such as proliferation, differentiation, and apoptosis but also their morphology, for instance, migration and adhesion [1]. Thus, a deep understanding of cell mechanical properties may significantly boost the fundamental studies of cell biology. To this end, many techniques including micropipette aspiration, atomic force microscope, magnetic twisting, and optical tweezers [2,3] have been developed. These techniques can perform the precise measurement of cell elasticity and promote the development of the field, but they are of limitations, such as low-throughput [2], or requiring expensive equipment [4]. Therefore, microfluidic technologies have been exploited for this purpose due to the advantages in single-cell manipulation with high-throughput, live-cell imaging, and precise control of microflow [5]. For example, the shear flows [6,7], extensional flows [8,9], or constriction channels [10–12] were produced in microfluidics to investigate cell deformability. The Young's modulus or the apparent viscosity of a cell squeezing through the constriction channel was able to calculate with the aid of mathematical models [13]. The pressure inducing cell deformation is a critical parameter to calculate cell stiffness using these models. To accurately measure the real-time changing pressure in the microchannel to precisely calculate the cell elasticity, a microfluidic chip integrated with a separation unit and pressure feedback system was developed by Chen et al. [14]. The K562 and human umbilical vein endothelial cells (HUVECs) were employed to demonstrate the cell elasticity measurement capability of the chip. The measured elasticity and fluidity of K562 and HUVEC cells were well consistent with previous studies.

This paper introduces the details of the fabrication of the microfluidic chip and the measurement process of cell elasticity. It aims to provide readers essential and detailed protocols to study the cell mechanical property using the microfluidic chip inducing large cell deformation.

Design of the microfluidic chip

The design of the chip is shown in Fig. 1a. The chip consists of 5 parts, a multi-level filtration unit (Fig. 1b), a separation unit (Fig. 1d), a constriction channel (Fig. 1c), two sensor-connection channels, and a winding channel. The inlet port is followed by the multi-level filtration unit consisted of 24 μm deep microchannels with the width ranging from 25 μm to 200 μm. Following the multi-level filtration, a separation unit including one straight main channel (24 μm deep) and 12 side channels (8 μm deep) evenly staggered on both sides was used to isolate rod- or flake-shaped particles from the cell suspension. As shown in Fig. 1d and e, the main channel is either 155 × 8 μm or 35 × 8 μm wide. The side channels staggered on both sides of the main channel eventually converge at the particle outlet at the right end of the chip. The main channel width gradually reduces from 155 μm to 6 μm with a depth of 16 μm to from the constriction channel (Fig. 1c). The constriction channel is 78 μm long and designed to deform living cells. The downstream winding channel measuring

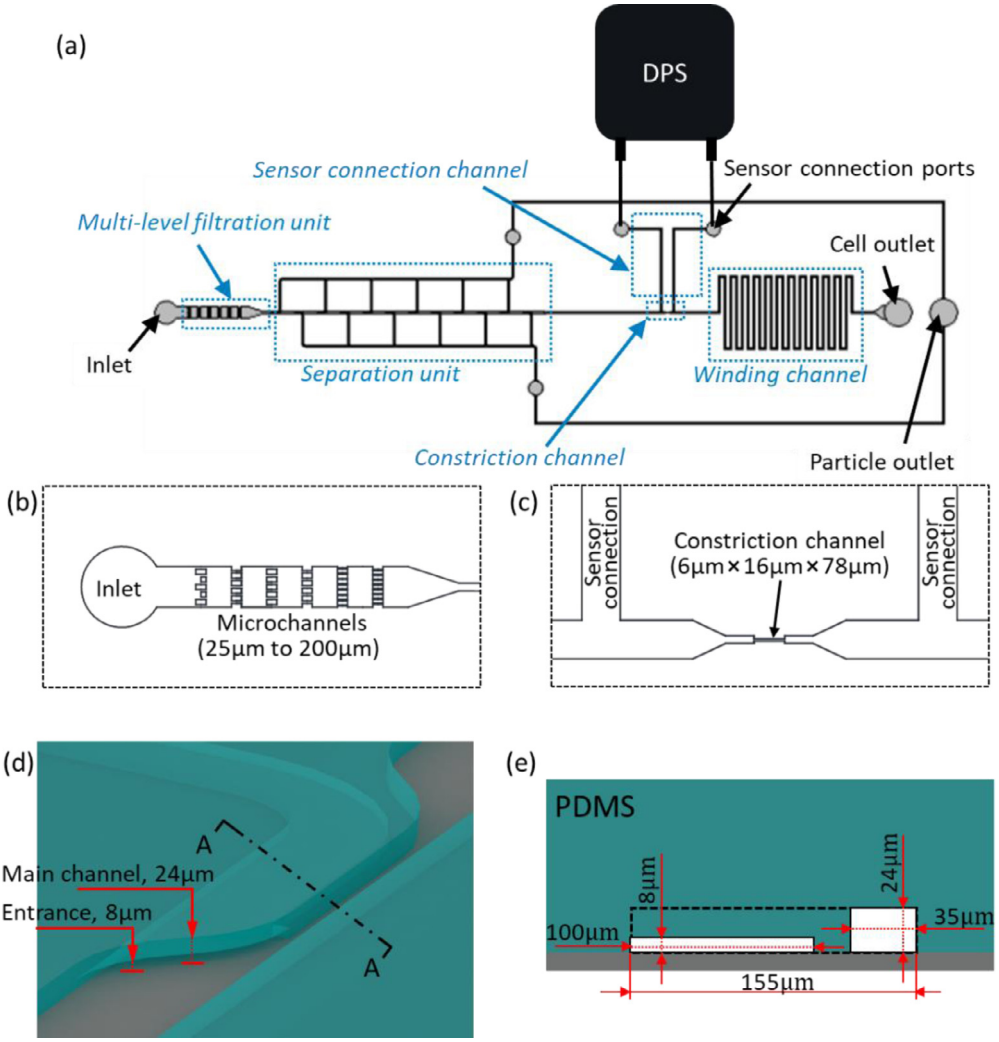

Fig. 1. The microfluidic chip design for cell elasticity measurement. Top view of (a) the whole device with the differential pressure sensor (DPS), (b) the multi-level filtration unit, and (c) the constriction channel. (d) An inset of the side channel entrance in the separation unit. (e) The cross-section of the main channel along line A-A in (d).

100 μm wide and 24 μm deep was employed to generated hydraulic resistance to adjust the pressure drop along with the whole device. The sensor-connection channels on either side of the constriction channel are 100 wide and 24 μm deep. They are connected to a differential pressure sensor (DPS) through tubing (Fig. 1a and c).

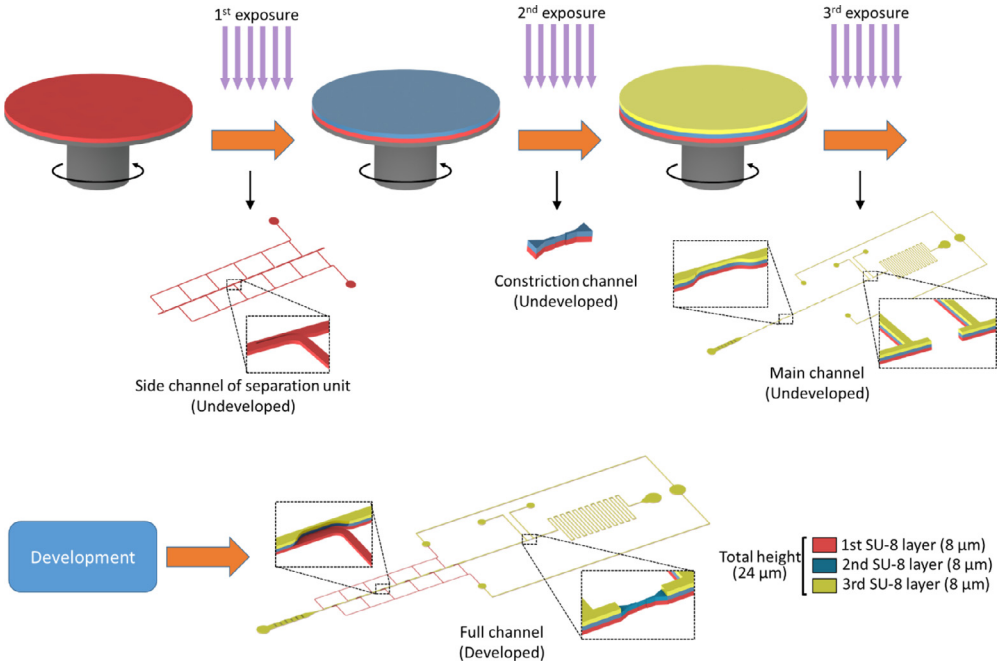

Fig. 2. The multiple-lithography process of the SU-8 mold for the microfluidic chip.

Device manufacture

The microfluidic chip was fabricated by standard soft lithography (Fig. 2) as described elsewhere [15–18]. After 30-minute dehydration at 200 °C, the wafer was spin-coated with SU-8 2007 (MicroChem, Newton, MA, USA) at 1800 rpm to obtain an 8 μm thick film (Fig. 2a). It was subsequently baked at 95 °C for 4 min on a hot plate within a fume hood. To form the 8 μm deep side channel of the separation unit, the wafer with an 8 μm thick film was exposed to UV light (URE-2000, Chinese Academy of Sciences, Beijing, China) for the first time with a dose of 120 mJ/cm^2 under a photomask with the side channel. The film was further baked at 65 °C for 3 min until the side channel of the separation unit appeared. Afterward, another 8-μm thick film was manufactured on the first layer by repeating the above spin-coating and heating steps (Fig. 2b). The wafer with double layers (16-μm thick) was exposed under a photomask with the constriction channel to form the 16 μm deep constriction channel, after precise alignment. It was then baked at 65 °C for 3 min again. After that, the manufacturing steps were repeated and the third exposure was taken to form the remaining 24-μm deep channels (Fig. 2c). Finally, the photoresist film was developed in SU-8 developer (MicroChem) and obtained the channel network with three different thicknesses (Fig. 2). After washing by isopropanol and dried by compressed nitrogen, it was exposed to the vapor of 1H,1H,2H,2H-perfluorooctyl (Aladdin®, Shanghai, China) trichlorosilane under vacuum for 15 min for silanization.

The polydimethylsiloxane (PDMS) mixture of Sylgard® 184 elastomer base and curing agent (Dow Corning®, USA) with the weight ratio of 10:1 was cast to the mold. After it was thoroughly degassed under a vacuum and baked in an oven at 60 °C for 2 h, the cured PDMS replica was peeled off from the mold. The replicas were punched with inlet, outlet, and sensor connection ports, before oxygen plasma treatment for 30 s with glass slides. Finally, the PDMS replicas were irreversibly boned to the glass slide.

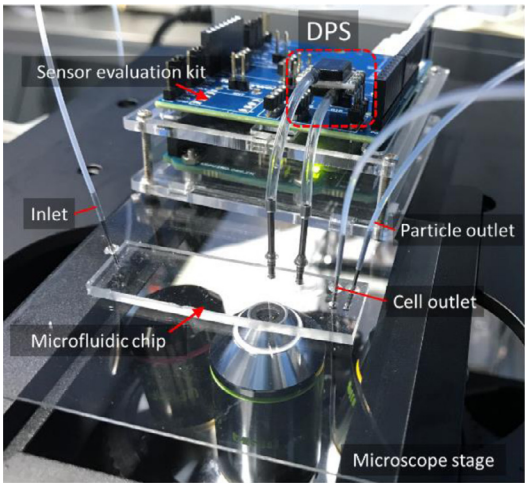

Fig. 3. The photo of the microfluidic device and the pressure feedback system on a microscope stage.

A DPS (HSCDRRN010ND6A3, Honeywell, New Jersey, USA) with a measurement range of ±2488.4 Pa and a resolution of 6.2 Pa was connected to the silicone tubing (I.D = 0.8 mm, O.D = 1.6 mm, ST004, SHENTONG, China). The DPS with tubing was then filled up with insulation oil (Yinglida, Shenzhen, China), before connecting to the sensor-connection ports.

Platform construction and experiment control

As shown in Fig. 3, the inlet, and outlet ports were connected to silicone tubing (I.D = 0.6 mm, O.D = 1.0 mm, ST039, SHENTONG, China) through 21-gage, flat-ended needles. The length of the outlet tubing on different devices is identical to ensure the same hydraulic resistance. The DPS was connected to the sensor-connection ports on the chip through 18-gage, flat-ended needles. The locations of the ports were shown in Fig. 1a. Then the DPS was mounted on a sensor evaluation kit (Honeywell, New Jersey, USA) with a microcontroller board (Arduino Uno Rev3), and then controlled by a computer program (Honeywell, New Jersey, USA) for pressure feedback with a sampling frequency of 5 Hz. A pressure pump (Elveflow, OB1 MK3+, Paris, France) was used to precisely control the pressure to drive either the inflow of cell suspension from the inlet or the outflow of the single cells to wastes. A 15-mL falcon tube with an airtight cap was connected to both the pressure pump and the inlet of the microchannel to provide cell suspension with 1000 cells per mL. The cell outlet was connected with another 15 mL falcon tube with an airtight lid for waste cell collection using negative pressure from the pump (ranges from −900 to 1000 mbar). The same connection is used at the particle outlet to maintain constant pressure. A constant pressure of −7500 Pa was provided at the cell outlet to draw cells to deform and pass through the constriction channel. The pressure at the particle outlet was kept at −1600 Pa to enhance the filtration efficiency of the separation unit. Finally, the microfluidic system was mounted on the stage of an inverted microscope (IX83 Olympus, Japan) equipped with a CCD camera (C11440–36 U, Hamamatsu, Japan) to image the deformation of cells in the constriction channel every 0.2 s.

Measurement and calculation process

A power-law rheology model was employed to interpret the cell deformation [14,19]. The cell protrusion $L_p(t)$ is a function of the pressure drop ($\Delta\bar{P}$) across the constriction channel, deformation

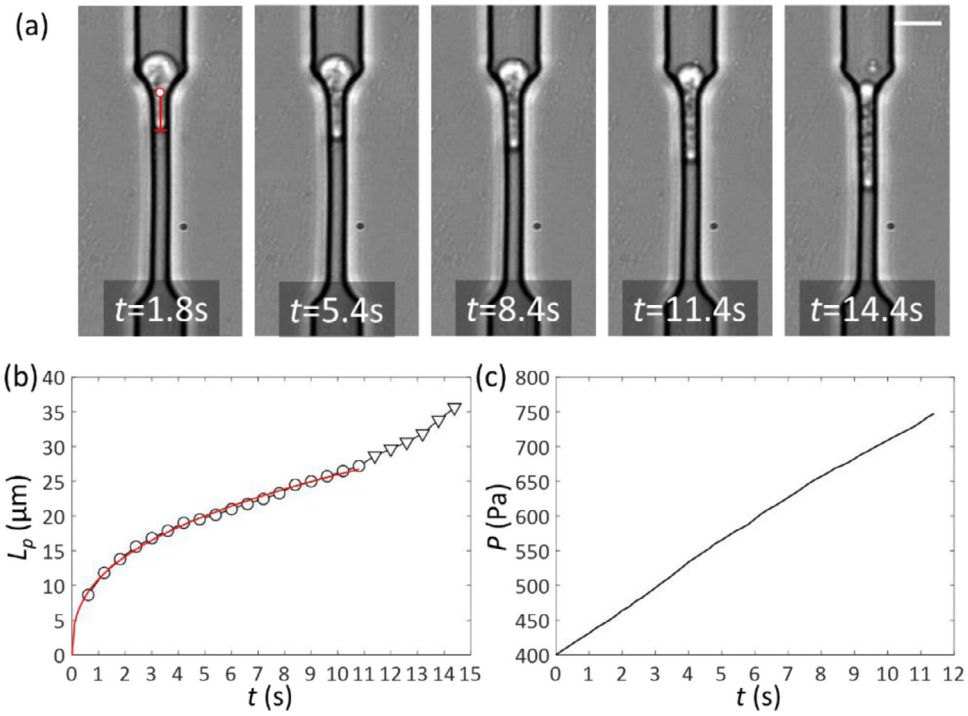

Fig. 4. The deformation process of a K562 cell. (a) The micro photos during the deformation. The protrusion is the length between the measurement origin (red circle) and the leading edge of the cell (red line). (b) The temporal variation of L_p during the deformation. Hollow triangles are the rapid deformation stage, and only hollow circles are employed to fit the power-law rheology model. The fitting curve of the model is red. (c) The temporal variation of pressure drop during the deformation. The scale bar on figure (a) is 20 μm.

time (t), and shear creep J(t). It is given by:

$$J(t) = \frac{2\pi}{\emptyset_p R_p} \frac{L_p(t)}{\Delta \bar{P}} \tag{1}$$

where R_P is the pipette radius (equivalent to the effective radius $R_{eff} = \sqrt{h \cdot w/\pi}$ [20]) and $\emptyset_P$ is a function of the ratio of the wall thickness to the radius of the pipette (usually 2.1 [21]).

The shear compliance constant (A_J) (Pa^{-1}) reflecting the deformability of the cell can be described by:

$$A_J = \frac{J(t)}{(t/t_0)^{\alpha}} \tag{2}$$

where α is the power-law exponent. It can vary from 0 to 1, reflecting elastic to viscous behavior.

Thus, cell protrusion ($L_p(t)$) is therefore given by:

$$L_p(t) = A_J \Delta \bar{P} \frac{\emptyset_p R_p}{2\pi} (t/t_0)^{\alpha} \tag{3}$$

Furthermore, the shear stiffness constant A_G (Pa) can be described by:

$$A_G = \frac{1}{A_J \Gamma(1+\alpha)} \tag{4}$$

where Γ is the gamma function. The A_G is equal to the Young's Modulus for $t = t_0 = 1$ s [19,22].

During the experiment, both the micrographs of the deformed cells and related pressure drop were simultaneously recorded using MicroManager [23] and the sensor evaluation kit, respectively.

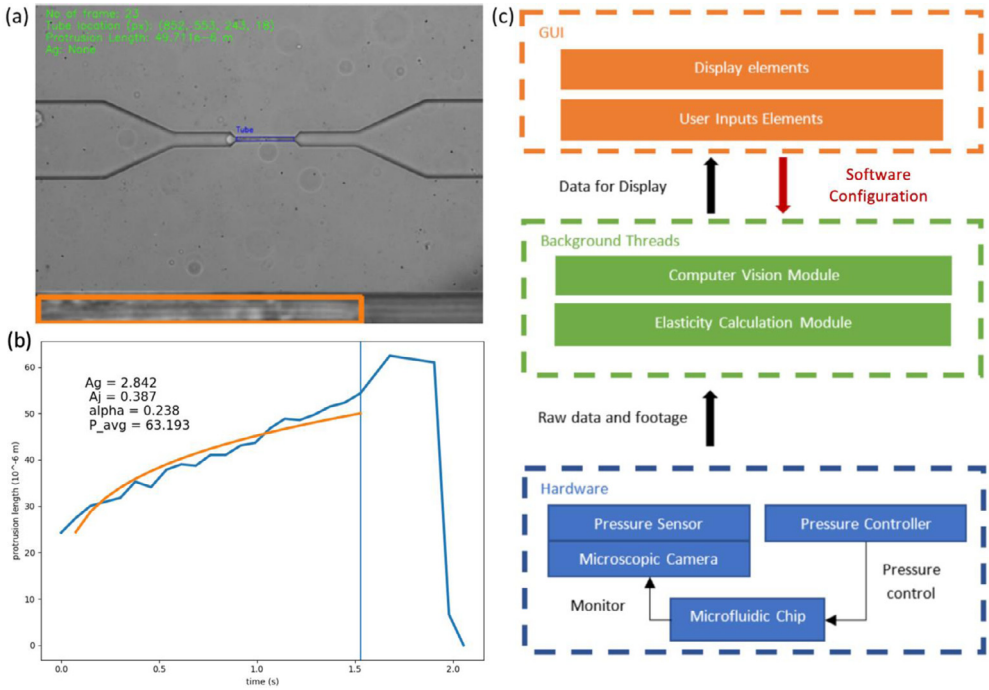

Fig. 5. Video processing software for real-time measurement of cell elasticity (a) The screen capture of the GUI of the offline prototype running. Real-time texts of various metrics (Green). Region of Interest (Blue). Cell detection bounding box (Orange). (b) The resultant protrusion length against time curve (Blue curve). The cutoff point of data filtering (Blue vertical). Logarithmic curve fitting (Orange). Metrics of interest (Black). (c) The architecture of the automated cell elasticity measurement software.

Afterward, images showing cell deformation were processed using ImageJ [24]. The protrusion length (Lp) at different times (t) during the deformation of the cell was acquired. As shown in Fig. 4a and 4b, the protrusion refers to the length between the measurement origin (the red circle) and the leading edge of a cell. It dramatically increased with time and a rapid deformation stage existence when the cell was almost fully squeezed into the channel. The protrusion data during the rapid deformation stage (t = 11.4 s - 14.4 s, triangles in Fig. 4b) was not considered in the power-law rheology model, since this stage was not described by Eq. (3). The instantaneous pressure drop ($\Delta P(t)$) inducing the cell deformation (Fig. 4c) was used to calculate the pressure ($\Delta\bar{P}$) in Eq. (3) by Lange et al. [20]

$$\Delta\bar{P} = 1/t_{total} \int \Delta P(t)dt \tag{5}$$

Finally, the data of L_p, t and $\Delta\bar{P}$ were fitted to Eq. (3) to acquire shear compliance constant (A_J) and exponent (α) of the cell.

Video processing software for cell elasticity measurement

A video processing software has been developed to automate the real-time detection of protrusion length of the cell in a constriction channel. Our python code utilizes the open source computer vision library OpenCV and other packages for reading logs and data stream of the pressure sensor. This program takes video of the cell movement across the constriction channel and simultaneous pressure data logs as inputs. Through the graphical user interface (GUI) of our software, the user is prompted to manually select the region of interest for cell recognition and length inference (the whole contraction channel in this case). After selection, the software runs, recognizes the cell as it moves across the

screen of the video and infers the protrusion length. The user can view the recognition results on a simple GUI window (Fig. 5a). The window displays the video frame, metrics of interest and cell recognition bounding box. When the cell exits, the prototype is triggered to calculate cell elasticity. The prototype is capable of extracting suitable data and performing curve-fitting on protrusion length-time curve. It reports to user with a saved plot of the curve with other metrics of interest, e.g. A_G and α (Fig. 5b).

The software architecture (Fig. 5c) consists of three layers, namely hardware, background threads and GUI. When a cell passes through the constriction channel, the equipment in the hardware layer would measure and stream the pressure data as well as the microscopic video frame of the channel to the background threads of the software. The threads would receive the data packets, calculate cell elasticity in real-time. The raw data and processed data packets would then be sent to the GUI for display. The GUI would handle user inputs and configuration, such as configuring hardware serial ports and selecting the region of interest.

Declaration of Competing Interest

The Authors confirm that there are no conflicts of interest.

Acknowledgments

The experiments were performed at the Center for Microflows and Nanoflows, Harbin Institute of Technology, Shenzhen. This work was supported by the National Natural Science Foundation of China (Grant No. 31701187) and the Shenzhen Science and Technology Innovation Committee (Grant No. JCYJ20180306172109024, JCYJ20170811160246740, and JCYJ20170413105329648).

References

[1] B. González-Bermúdez, G.V. Guinea, G.R. Plaza, Advances in micropipette aspiration: applications in cell biomechanics, models, and extended studies, Biophys. J. 116 (4) (2019) 587–594.
[2] R.M. Hochmuth, Micropipette aspiration of living cells, J. Biomech. 33 (1) (2000) 15–22.
[3] I.L. Ahmad, M.R. Ahmad, Trends in characterizing single cell's stiffness properties, Micro Nano Syst. Lett. 2 (1) (2014) 8.
[4] A. Fontes, M.M. Brandão, M.L. Barjas-Castro, L.C. Barbosa, F.F. Costa, C.L. Cesar, S.T.O. Saad, Optical tweezers for measuring red blood cell elasticity: application to the study of drug response in sickle cell disease, Eur. J. Haematol. 70 (2003) 207–211.
[5] A. A.P. Ravetto, C.V.C. Bouten, J.M.J. den Toonder, Microfluidics for single cell mechanical characterization: a review, SM J. Biomed. Eng. (2017).
[6] A.M. Forsyth, J. Wan, W.D. Ristenpart, H.A. Stone, The dynamic behavior of chemically "stiffened" red blood cells in microchannel flows, Microvasc. Res. 80 (1) (2010) 37–43.
[7] N. Korin, A. Bransky, U. Dinnar, Theoretical model and experimental study of red blood cell (RBC) deformation in microchannels, J. Biomech. 40 (9) (2007) 2088–2095.
[8] D.R. Gossett, H.T. Tse, S.A. Lee, Y. Ying, A.G. Lindgren, O.O. Yang, J. Rao, A.T. Clark, D. Di Carlo, Hydrodynamic stretching of single cells for large population mechanical phenotyping, Proc. Natl. Acad. Sci. U.S.A. 109 (20) (2012) 7630–7635.
[9] S.S. Lee, Y. Yim, K.H. Ahn, S.J. Lee, Extensional flow-based assessment of red blood cell deformability using hyperbolic converging microchannel, Biomed. Microdevices 11 (5) (2009) 1021–1027.
[10] S. Gabriele, A.M. Benoliel, P. Bongrand, O. Théodoly, Microfluidic investigation reveals distinct roles for actin cytoskeleton and myosin II activity in capillary leukocyte trafficking, Biophys. J. 96 (10) (2009) 4308–4318.
[11] H.W. Hou, Q.S. Li, G.Y.H. Lee, A.P. Kumar, C.N. Ong, C.T. Lim, Deformability study of breast cancer cells using microfluidics, Biomed. Microdevices 11 (3) (2009) 557–564.
[12] M.J. Rosenbluth, W.A. Lam, D.A. Fletcher, Analyzing cell mechanics in hematologic diseases with microfluidic biophysical flow cytometry, Lab Chip 8 (7) (2008) 1062.
[13] C.T. Lim, E.H. Zhou, S.T. Quek, Mechanical models for living cells—A review, J. Biomech. 39 (2) (2006) 195–216.
[14] Z. Chen, Y. Zhu, D. Xu, M.M. Alam, L. Shui, H. Chen, Cell elasticity measurement using a microfluidic device with real-time pressure feedback, Lab Chip 20 (13) (2020) 2343–2353.
[15] H. Chen, J. Sun, E.J. Wolvetang, J.J. Cooper-White, High-throughput, deterministic single cell trapping and long-term clonal cell culture in microfluidic devices, Lab Chip 15 (4) (2014) 1072–1083.
[16] H. Chen, C. Chen, S. Bai, Y. Gao, G. Metcalfe, W. Cheng, Y. Zhu, Multiplexed detection of cancer biomarkers using a microfluidic platform integrating single bead trapping and acoustic mixing techniques, Nanoscale 10 (43) (2018) 20196–20206.
[17] Z. Chen, Y. Zhu, D. Xu, M.M. Alam, L. Shui, H. Chen, Cell elasticity measurement using a microfluidic device with real-time pressure feedback, Lab Chip (2020).
[18] C. Chen, D. Xu, S. Bai, Z. Yu, Y. Zhu, X. Xing, H. Chen, Dynamic screening and printing of single cells using a microfluidic chip with dual microvalves, Lab Chip 20 (7) (2020) 1227–1237.

[19] E.H. Zhou, S.T. Quek, C.T. Lim, Power-law rheology analysis of cells undergoing micropipette aspiration, Biomech. Model Mechanobiol. 9 (5) (2010) 563–572.
[20] J.R. Lange, J. Steinwachs, T. Kolb, L.A. Lautscham, I. Harder, G. Whyte, B. Fabry, Microconstriction arrays for high-throughput quantitative measurements of cell mechanical properties, Biophys. J. 109 (1) (2015) 26–34.
[21] M.J. Levesque, D.P. Theret, M. Sato, R.M. Nerem, L.T. Wheeler, The application of a homogeneous half-space model in the analysis of endothelial cell micropipette measurements, J. Biomech. Eng. (1988) 110.
[22] K.D. Nyberg, K.H. Hu, S.H. Kleinman, D.B. Khismatullin, M.J. Butte, A.C. Rowat, Quantitative deformability cytometry: rapid, calibrated measurements of cell mechanical properties, Biophys. J. 113 (7) (2017) 1574–1584.
[23] A. Edelstein, N. Amodaj, K. Hoover, R. Vale, N. Stuurman, Computer control of microscopes using μmanager, Current Protocols Mol. Biol. 92 (1) (2010).
[24] C.A. Schneider, W.S. Rasband, K.W. Eliceiri, NIH Image to ImageJ: 25 years of image analysis, Nat. Meth. 9 (7) (2012) 671–675.